# Heterogeneous distribution of metal nanocrystals in glazes of historical pottery

I. Borgia[a], B. Brunetti[a,*], I. Mariani[a], A. Sgamellotti[a], F. Cariati[b],
P. Fermo[b], M. Mellini[c], C. Viti[c], G. Padeletti[d]

[a]INSTM and Dipartimento di Chimica, Università di Perugia, Via Elce di Sotto 8, 06123 Perugia, Italy
[b]INSTM and Dipartimento CIMA, Università di Milano, Via Venezian 21, 20133 Milan, Italy
[c]Dipartimento di Scienze della Terra, Università di Siena, Via Laterina 8, 53100 Siena, Italy
[d]CNR-ICMAT, Via Salaria Km. 29,300, CP 10, 00016 Monterotondo Stazione, Rome, Italy

## Abstract

It has been recently shown that lustre decoration of medieval and renaissance pottery consists of silver and copper nanocrystals, dispersed within the glassy matrix of the ceramic glaze. Lustre surfaces show peculiar optical effects such as metallic reflection and iridescence. In many cases, lustre appears overlapped to colored drawings. Here we report the findings of a study on glazes, pigments and lustre of several shards belonging to Deruta and Gubbio pottery of XVI century. The components of glazes and pigments have been identified. Lustre is confirmed to be characterised by silver and copper metal nanocrystals inhomogeneously dispersed in the glassy matrix of the glaze. In the case of lustre overlapped to colored decorations, we found two contradictory cases. The first consists of a lustre surface successfully applied over a blue smalt geometrical drawing. The second consists of a lustre surface, unsuccessfully applied over a yellow lead-antimonate pigment. The yellow pigment hinders the formation of lustre and removes crystals of tin dioxide, normally present in the glaze as opacifier. © 2002 Elsevier Science B.V. All rights reserved.

## 1. Introduction

Lustre was one of the most important decorative techniques of medieval and renaissance pottery of the Mediterranean basin. It consisted of a metal deposition on a tin-opacified lead glaze which produced brilliant reflections of different colors and iridescence [1]. Historically, lustre was first used during IX century A.D. to decorate pottery of Mesopotamia. The technique, later used in Egypt during the Fatymid period (X century), spread all along the Mediterranean basin together with the diffusion of Islamic culture (X–XIV century). Lustre decorations reached their maximum development first in Spain, from XIV to XVI century, with the productions of Paterna and Manises, and later in Italy, from XV to XVI century, with the manufactures of Deruta and Gubbio, where lustre was used to

* Corresponding author. Tel.: +39-75-5855509;
fax: +39-75-5855606.
E-mail address: bruno@dyn.unipg.it (B. Brunetti).

decorate the finest polychrome pottery of the Italian renaissance [1–4].

Lustre was prepared through a procedure consisting of a ''third firing'' deposition of a thin film of copper and silver crystals onto the surface of a previously glazed and decorated pottery. The deposition was applied with the brushing over of a mixture of silver, copper, and iron salts or oxides, together with vinegar and additional substances. The temperature was then raised to approximately 600 °C and a reducing atmosphere was produced. In these conditions: (a) glaze softened; (b) silver and copper compounds were reduced to metals; (c) metal was deposited within the outer layers of the glaze, which remained trapped there [5,6].

Surprisingly, recent work demonstrated that lustre consists of a heterogeneous metal–glass composite film, some hundreds of nanometres thick, analogous to that present in the modern metal–glass nanostructured composites, obtained by ion implantation, ion-exchange or sol–gel deposition on pure silica matrices, followed by annealing under reducing atmosphere [7–9]. In the lustre, separate silver and copper pseudo-spherical nanocrystals appear to be dispersed within the outer layers of the glaze [7]. Although overall heterogeneous, the nanocrystal distribution can be locally homogeneous, being characterised, in specific regions, by constant dimensions and constant density of nanocrystals. However, crossing the lustre layer towards the ceramic support, the nanocrystal dimensions decrease from tens of nanometres to a few nanometres [7].

The optical properties of lustre are connected with the specific nanostructures of the silver and copper depositions [8–10]. Nevertheless, they are expected to be also dependent on copper–silver ratio, on the nature of the glaze and, when applied over pre-existing pigments, on the interaction with the underlying colors.

Here we discuss the results of a study accomplished on several shards of Italian renaissance lustre pottery from Deruta and Gubbio. All the samples show the typical tin-opacified lead glazes decorated with blue drawings and gold lustre. However, some of them also show rich and polychrome decorations with blue and yellow-orange drawings together with gold, red, and copper-like lustre. These fragments, belonging to renaissance ceramics from Gubbio (XVI century),

show the interesting case of two different attempts to produce lustre reflection and iridescence, over-lapped to a previously pigmented base. The first example is a common transparent lustre layer over-imposed on a blue geometrical drawing, the second is a (failed) lustre decoration overimposed on a yellow-orange flower.

The study widely confirms that lustre is composed of heterogeneous distributions of copper and silver nanocrystals and shows that ancient masters were continuously experimenting for new effects in decorations.

## 2. Experimental

Analytical investigations were performed using scanning electron microscopy with energy dispersion X-ray spectrometry (SEM–EDX), transmission electron microscopy with energy dispersion X-ray spectrometry and selected area electron diffraction (TEM–EDX–SAED), and Vis–UV reflectance spectroscopy.

SEM images, formed using back-scattered electrons (BSE), and EDX analyses have been taken by a Philips XL30 with an $LaB_6$ source and an EDAX/DX4 detector.

TEM images, EDX analyses and SAED patterns have been recorded using a Jeol 2010 operating at 200 kV and having a theoretical point-to-point resolution of 1.9 Å. The EDX spectrometer is equipped with an ultra-thin window, capable to detect elements heavier than boron. Electron-transparent sections were obtained using a Gatan dual ion mill thinner (argon ions).

Vis–UV reflectance spectra have been recorded using a JASCO UV/Vis/NIR spectrophotometer model V-570 equipped with a barium sulfate integrating sphere.

## 3. Results and discussion

### 3.1. The glazes

The analyses of the glazes of all the samples indicated that they have the typical composition of the opacified lead glazes, used by Italian masters to produce lustre pottery in XV and XVI century. Typical

compositions, as semi-quantitatively determined by averaging on repeated SEM–EDX analyses performed on large selected areas are $SiO_2$, 45–65 wt.%; PbO, 15–35 wt.%; $Na_2O$, 1–3 wt.%; $K_2O$, 5–9 wt.%; $Al_2O_3$, 2–5 wt.%; CaO, 1–5 wt.%; MgO, 0–0.5 wt.%; FeO, 0.5–2.5 wt.%; $SnO_2$, 5–9 wt.%. As already remarked in [7], these glazes show a lower lead oxide content and a relatively larger quantity of alkali, compared to the typical glazes for Hispano–Islamic lustre pottery of XIV and XV century.

### 3.2. The pigments

All the examined samples show brilliant gold lustre and blue geometrical drawings. Some of them are polychrome and show lustre and pigments of different colors. As an example, Fig. 1 shows one of the Gubbio samples containing gold, red and copper-like lustre, together with blue drawings and a yellow-orange decoration consisting of a flower. Although poorly evident in the picture, lustre reflection and iridescence are fully attained, when applied over the white-opacified glaze. A brilliant (copper-like) lustre is also attained, when applied over the blue pigment. Conversely, the yellow-orange flower of Fig. 1 shows evident lustre metallic reflection only at its borders. Apparently, the lustre preparation mixture was applied all over the colored flower. However, lustre was attained only around the flower on the region of pure glaze, where no yellow pigment was present.

As shown in the following, the study of the two pigments indicated that the blue pigment is smalt, while that orange-yellow is lead-antimonate (or *Giallo di Napoli*). Both pigments were commonly used to decorate medieval and renaissance ceramics [6,11,12].

#### 3.2.1. The blue smalt

Smalt is an artificial pigment, consisting of a potassium silicate glass with some cobalt oxide. Old recipes indicate that smalt was prepared first roasting a complex Co–Ni–Fe–As ore, most of the arsenic volatilized during roasting, then cobalt, nickel and iron oxides were melted together with siliceous sand [11]. Since ancient times, smalt was used to color and decorate glasses, but powdered cobalt glass was also used as painter pigment. For instance, it was largely used by Italian painters of XIV and XV century, as shown in several cases [13,14].

The blue smalt of Deruta renaissance pottery has already been characterised, in our laboratory, in a previous work performed on different samples, by micro-X-ray fluorescence (XRF), XRF with secondary anode, and SEM–EDX [15]. Here the analyses have been carried out simply by SEM–EDX on cross-sections. Fig. 2 shows the typical EDX spectrum of the blue smalt, with evident peaks of Fe, Co and Ni. Ni
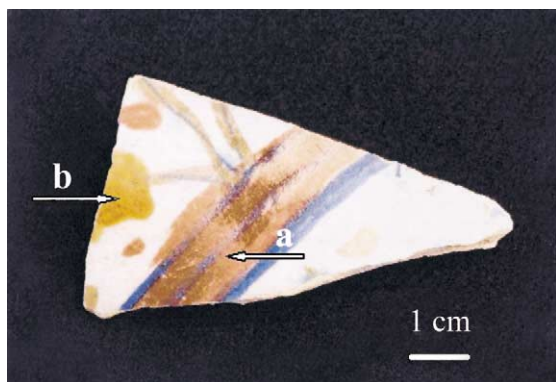


Fig. 1. Sample of a XVI century pottery from Gubbio, containing gold, red and copper-like lustre, together with blue geometrical drawings (a) and a yellow-orange decoration representing a flower (b). Although not clearly visible in the picture, a brilliant gold lustre is present all around the flower (b).
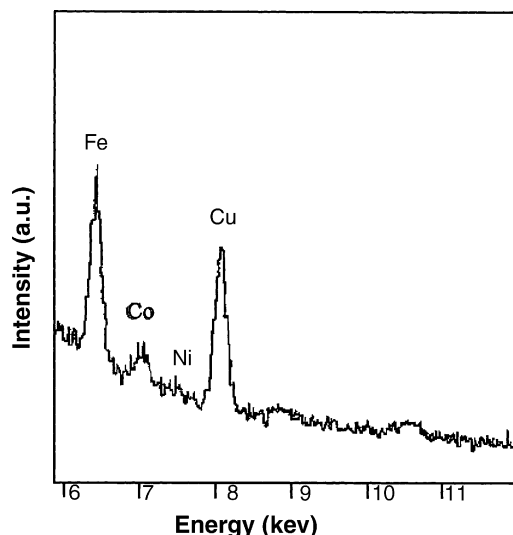


Fig. 2. SEM–EDX spectrum of a blue smalt geometrical drawing. The presence of copper is due to the lustre overlapped to the blue geometrical drawing.

and Co are typical elements of the pigment, whereas Fe can be a constituent of both the glaze and pigment. Actually, the presence of Fe in the smalt could be attributed to residues of iron oxide from the mixture applied to the surface to produce the lustre deposition. Some of the smalt SEM–EDX spectra, such as that reported in Fig. 2, show a Cu peak, but this signal was present only in those regions where lustre was overlapped to the blue pigment. Arsenic was not easily found. However, careful SEM observations revealed that crystals of a Ca–Pb–arsenate (Ca:Pb:As close to 30:30:40 at.%) show often association to the blue smalt in the glaze. The arsenate crystals are up to 10 µm in size and showed a typical hexagonal habit. The occurrence of arsenate crystals reasonably indicates incomplete As roasting.

The blue smalt was also spectroscopically identified by visible reflectance measurements. A spectrum is reported in Fig. 3, where the d → d band, peaked at about 600 nm, typical of the electronic spectrum of smalt, clearly appears. The band is structured in the three sub-bands originated by Jahn–Teller split transitions $^4A_2 \rightarrow ^4T_1(P)$ in a tetrahedral coordination [16].

### 3.2.2. *The yellow-orange lead-antimonate*

Lead-antimonate yellow, also known as *Giallo di Napoli*, was frequently used in the manufacturing of Italian renaissance ceramics, as reported by Piccolpasso [6]. It is an artificial pigment that has been manufactured in various periods; dating from XV century B.C., it was the only yellow colorant and opacifier in ancient and Mesopotamian glasses. The most common recipe for its preparation indicates that a mixture of lead and antimony oxides were roasted at high temperature [11]. The final color varied from yellow to orange according to the percentage of the two combined oxides [17]. In this study, the identification of the pigment was accomplished by SEM–EDX and by TEM–EDX. Fig. 4 reports two BSE–SEM cross-section images, taken at different magnification. The images well emphasize the large variety of dimensions of the euhedral crystals (between 0.5 and 10 µm) containing Pb, Sb and oxygen, as observed by EDX (Pb : Sb = 3 : 2). The chemical composition and the crystalline nature of the pigment were confirmed by TEM–EDX and by electron diffraction. A TEM image of small crystals, with about 500 and 800 nm size, is reported
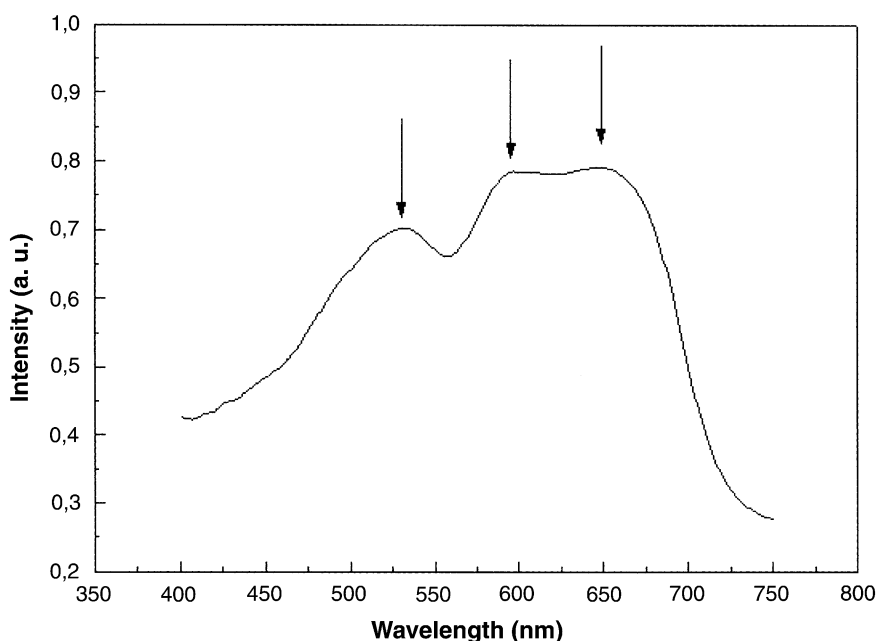
Fig. 3. Spectrum of a blue smalt drawing as recorded by visible reflectance measurements, using a barium sulfate integrating sphere. Arrows indicate the typical bands of the pigment (see text).
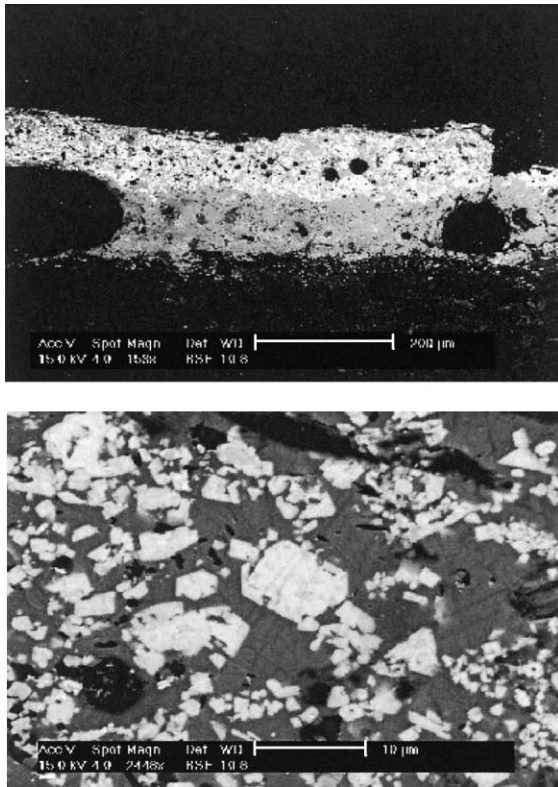
Fig. 4. BSE–SEM images of lead-antimonate crystals, taken at different magnification. The hexagonal crystals are 0.5–10 μm in size.



Fig. 5. TEM image (a), TEM–EDX spectrum (b) and electron diffraction pattern (c) of lead-antimonate crystals.

in Fig. 5, together with the corresponding EDX spectrum and SAED pattern.

### 3.3. The lustre

Lustre was present in all the examined samples. All the shards showed gold lustre, while some of them, as the one reported in Fig. 1, also showed red and copper-like metallic reflections.

As previously mentioned, it has been surprisingly found that lustre consists of a very thin heterogeneous film of metal nanocrystals dispersed in the glassy matrix of the glaze [7]. In this work, detailed TEM images of the lustre layer allowed us to confirm that lustre has a nanostructural metallic nature, which shows, in case of gold lustre, well-separated silver and copper quasi-spherical nanocrystals of variable diameter, approximately between 5 and 50–100 nm.
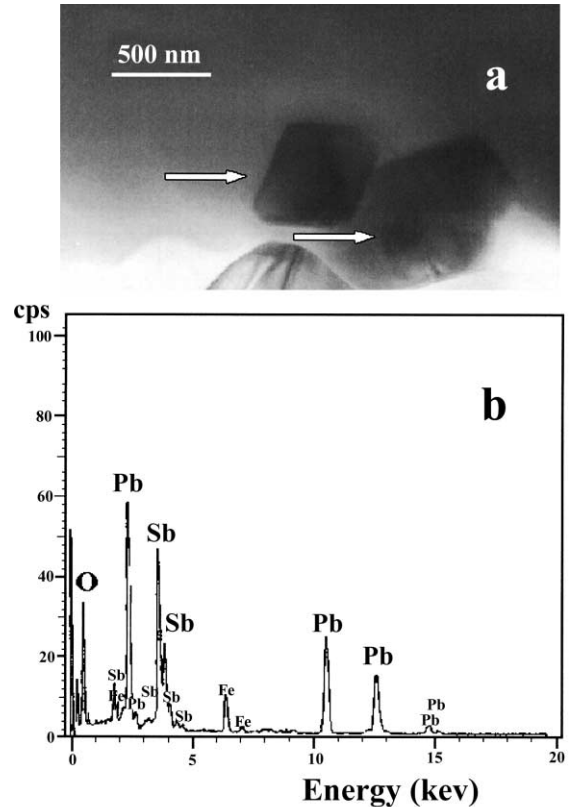
As already reported in [7], silver and copper crystals are well separated. In general, silver nanocrystals appear grouped together, to form clusters among a large number of copper crystals, and are characterised by larger average dimensions than those of copper. A typical situation is shown in Fig. 6, where the larger and darker crystals are observed as silver, while the others are copper. The typical distribution of silver
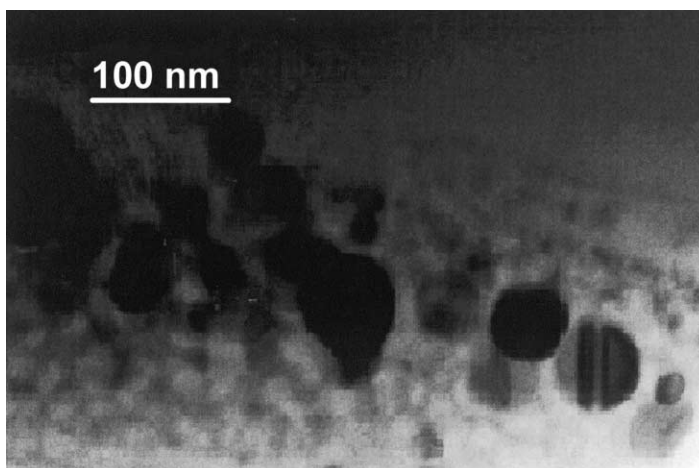
Fig. 6. TEM image of silver nanocrystals of about 40 nm diameter (black), among smaller (5–10 nm diameter) crystals of copper (grey).

among copper is also shown in Fig. 7, where the SEM distribution map of the two elements, taken selecting specific lines of the X-ray emission, is reported. Although the presence of silver was previously identified by EDX [7], this is a first direct TEM observation of silver nanocrystals in lustre decorations. It is worth noting that silver is characterised by nanocrystals that are distributed in regions close to the glaze surface.

A peculiar property of the lustre is the high density of the pseudo-spherical metal nanocrystals and their locally homogeneous distribution. To explain this point, a typical TEM micrograph of copper nanocrystals is reported in Fig. 8, together with the corresponding SAED pattern. The image shows a homogeneous distribution of nanocrystals, with an average diameter ~10 nm. The nanocrystals are randomly oriented and some of them show the copper lattice fringes.

The presence of copper and silver nanocrystals can also be identified by Vis–UV reflection spectroscopy measurements. In fact, absorption spectra of glass–metal nanostructured composites are known to show the typical surface plasmon resonances (SPRs) of metal nanoclusters dispersed in a glassy medium [9]. In Fig. 9, a typical Vis–UV absorption spectrum of a gold lustre layer present in one of our samples is shown. In the spectrum, both the SPR of silver (around 440 nm) and that of copper (around 560 nm) are clearly visible. It is known that the peak of the typical silver SPR is at a wavelength around 400 nm which,

however, can be shifted towards higher wavelength, as in this case, according to the dimensions of nanocrystals and glaze composition.

### 3.3.1. Lustre distribution over blue smalt

Well-formed gold and copper-like lustre decorations were frequently found in our samples overlapped with blue geometrical drawings. As discussed, smalt pigment consists of a potassium silicate glass with some cobalt. The glassy nature allows easy dispersion of the smalt into the glaze, from which appears its typical color, yet this does not modify other properties. The quantity of cobalt oxide necessary to get the blue color is very low; it is well established that 0.01% of CoO is sufficient to produce a deep blue [11]. Low concentration blue smalt, well dispersed in the glaze, does not significantly disturb lustre deposition. Behind the clearly visible metallic reflection, the presence of a well-formed lustre overlapped on the pigment is confirmed by the Cu peaks present in the corresponding SEM–EDX spectra. Moreover, the Vis–UV spectrum of Fig. 10, which refers to a region where gold lustre was overlapped on a blue drawing, further confirms the nanocrystalline nature of the lustre. Both the typical features of the gold lustre and the blue pigment are clearly evident. In particular, the SPR of silver at 440 nm is evident, demonstrating the success in nanocrystal formation. On the other hand, the typical SPR of copper nanocrystals at 560 nm is not visible, but only because of the significantly overlapped large
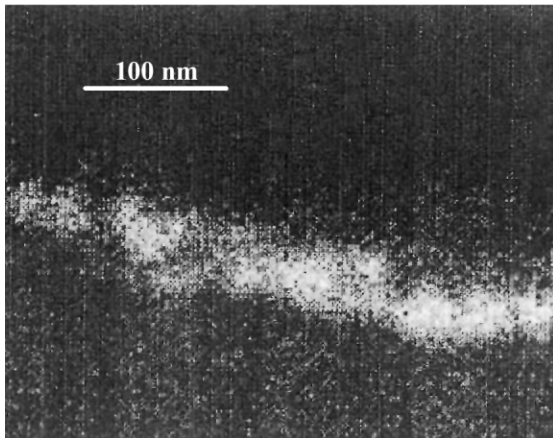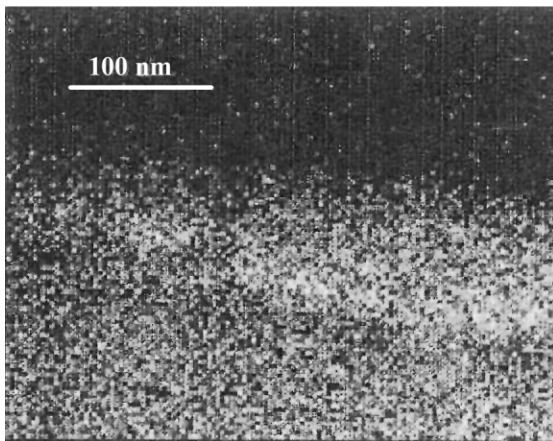
## Ag Lα



## Cu Kα



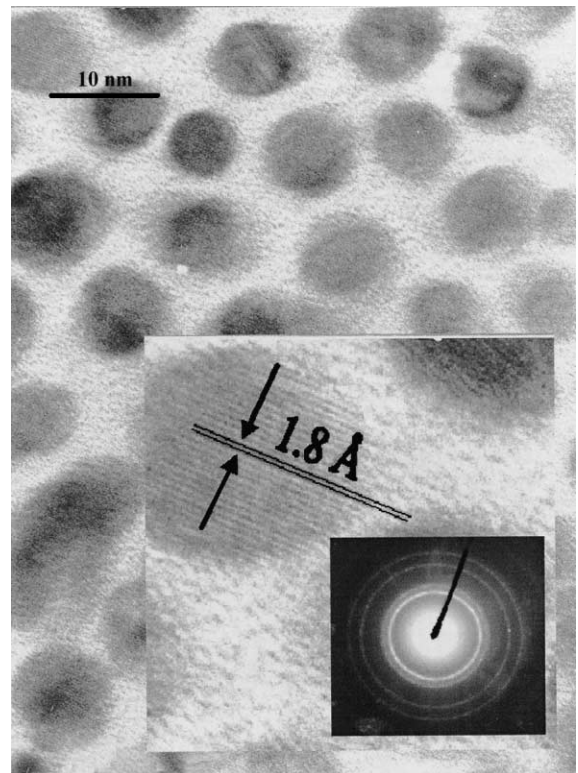Fig. 7. Distribution maps of elemental silver and copper in the lustre.



Fig. 8. Copper nanocrystals of about 10 nm diameter in a region of local homogeneity of the lustre deposition. The first inset shows a magnification of a 7 nm diameter crystal, with visible copper lattice fringes. SAED pattern identifies the crystals as metallic copper (second inset).

band from 550 to 750 nm, typical of the blue pigment spectrum (see Fig. 3).

### 3.3.2. Antimonate distribution and lustre

In the case of the orange-yellow flower, lustre effect was not attained over the flower but only over the white glaze, immediately close to the pigmented region. In fact, a careful inspection of the yellow flower maintains the evidence that lustre deposition was also attempted on the flower but without any success.

First of all, at a simple visual inspection, a brilliant gold lustre is present at the border of the yellow flower, but it does not abruptly finish when the yellow flower begins, showing a gentle decrease up to its disappearance. Second, accurate BSE–SEM observations indicate that few silver crystals are sometimes present in the yellow flower region, but only in the rare and small areas which appear fully free from lead-antimonate crystals. To support this view, in Fig. 11 it is reported a BSE–SEM image of a cross-section of a region where silver clusters are present over the yellow flower, far from its border. The image makes evident the presence of the lead-antimonate crystals and the presence of small silver crystals, identified by EDX, close to the glaze surface, but only in the small region free from the lead-antimonate.

As already shown in Fig. 4, lead-antimonate crystals are large (up to 10 μm) and deeply penetrated into the glaze. Their intrusion apparently produces significant alterations of the glaze surface, hindering the formation of the lustre.
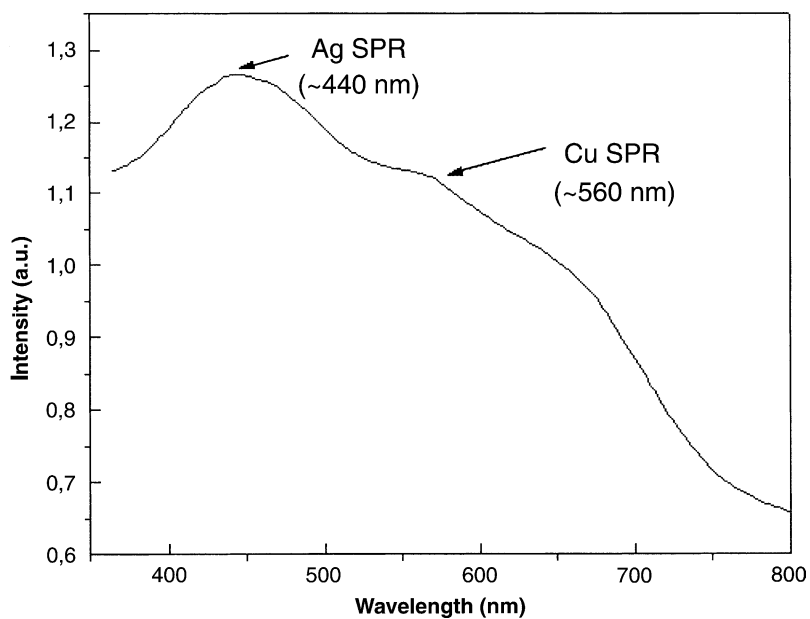
Fig. 9. Absorption spectrum of a gold lustre decoration as recorded by visible reflectance measurements. The SPRs of silver and copper nanocrystals dispersed in the glassy matrix of the glaze are indicated.
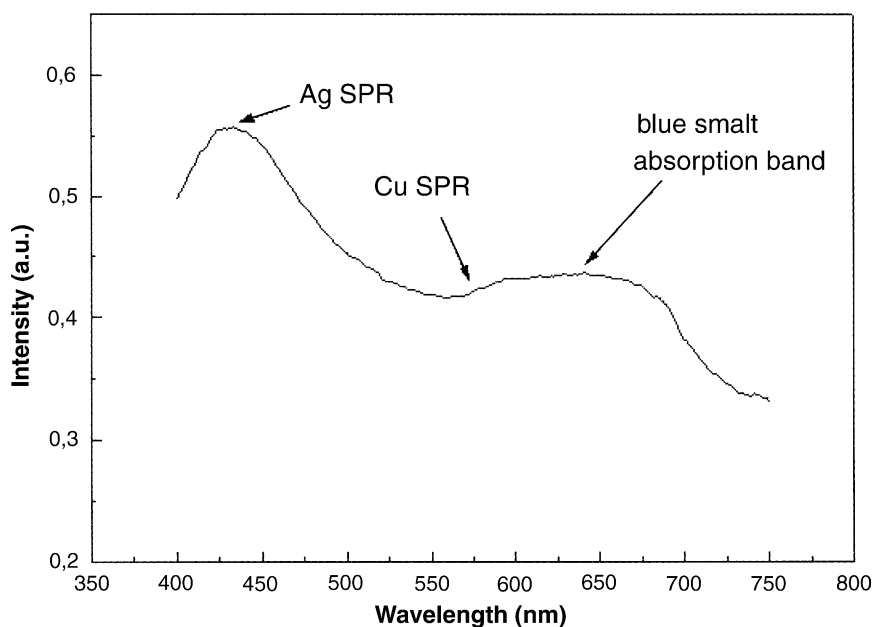


Fig. 10. Absorption spectrum of a gold lustre overlapped to a blue geometrical drawing as recorded by visible reflectance measurements. The SPR of dispersed silver and copper nanocrystals are indicated. The copper SPRs appears overlapped to the large absorption band of the blue smalt pigment.
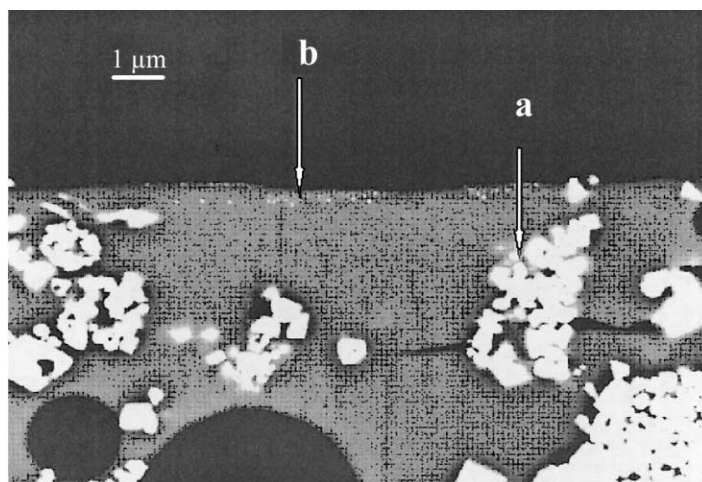
Fig. 11. BSE–SEM image of the region of the yellow flower far from the border characterised by the presence of brilliant gold lustre. The image puts clearly in evidence the presence of the lead-antimonate crystals (a) and the presence of small silver crystals (b) identified by EDX, close to the glaze surface where lead-antimonate is lacking.

The yellow pigment crystals produce further modifications of the glaze properties. Tin dioxide, as cassiterite, is normally present in the glaze as opacifier. However, SEM–EDX analyses in the region of the antimonate pigment did not show any presence of tin, being tin present in the surrounding parts. Therefore, we conclude that application of the pigment moved tin dioxide towards the adjacent regions or, alternatively, that the presence of antimonate passivated the tin dioxide recrystallization. To understand this point, we remind that, when glaze is fired, tin dioxide first melts within the lead silicate, in the temperature range 600–650 °C; then, in the range 700–750 °C, starts to recrystallize and remains crystalline during heating up to and cooling down from 1200 °C [18].

### 3.3.3. Comment on lustre formation

As mentioned in Section 1, a strong analogy exists between composition and microtexture of lustre and that of silicate glasses containing metal clusters, which have attracted interest in recent years as materials for non-linear optical device fabrication [8]. Therefore, although the nanocluster formation mechanism in a glassy matrix is still under debate, some simple considerations on lustre formation can be drawn on the basis of the recent studies on metal nanocrystals, produced in ion-bombarded pure silica [19], in sol–gel depositions on silica [20], or in silver–sodium

exchanged glasses [21], thermally treated in a reducing atmosphere. Most of these studies have been recently carried out to study the physics and the chemistry of nanocrystal formation, the crystal structure and properties, the crystal–matrix interaction and the general metal–glass composite properties for optoelectronics applications. It has been found that the structure, size and size distribution of nanocrystals mainly depend on the nature of the ions and their interaction with the matrix and the environment, while the aggregation behavior is determined by the temperature and by the electronic, thermal and structural properties of the glass and the ions [22].

In spite of the complex nature of nanocrystal formation mechanism, following the indications of these works, it appears quite reasonable that the first step of lustre formation consists of an ion-exchange between the alkali ions present in the glaze [7] and silver and copper ions present in the mixture of the lustre recipe [6]. The second step could then be the reduction of the ions, as produced by thermal annealing and/or by reducing atmosphere.

Actually, silver–sodium and copper–sodium ion-exchange has been documented to occur efficiently at the surfaces of glasses immersed in a molten salt mixture, even for low salt concentration [21] and the ion-exchange technique has been successfully applied to develop special glasses with high specific proper-

ties, by replacing alkali ions with other monovalent cations [22]. First crystal nucleation is, therefore, expected to be originated by a spontaneous reaction of the ions in the matrix, as produced by an external reducing agent, possibly created in the kiln by the introduction of smoking organic substances, at about 600 °C [6,7]. In fact, recent experimental evidences has shown that $Ag^+$ and $Cu^+$ ion-implanted or ion-exchanged glasses, at around 600 °C in a reducing atmosphere (5% $H_2$ in $N_2$), easily produce metal nanoclusters [11,23,25]. After the first nucleation, the growth can be regarded as a process due to the supersaturation of the crystal constituent concentrations in the region where clustering occurs [24,26].

Although certainly oversimplified, this description rationalizes the results obtained in this work and in the recent study on lustre surfaces in Spanish and Italian pottery from XIV to XVI century [7]. In particular, this description allows us to explain the lacking lustre in the yellow pigment region as due to the large yellow pigment crystals which obstacle the primary alkali-silver/copper ion exchange, thus avoiding a significant nucleation and growth of metal nanocrystals. Conversely, the process is not hindered by the glassy blue smalt, due to its diffusion into the glaze and low concentration.

## 4. Conclusion

In conclusion, an extended study has been carried out on several samples of medieval and renaissance lustre pottery from Deruta and Gubbio.

The glaze shows the typical composition used by Italian masters for lustre depositions, with the presence of a relatively larger quantity of alkali compared to the glazes of Hispano–Islamic lustre pottery.

Lustre is confirmed to be characterised by a heterogeneous distribution of silver and copper nanocrystals, which, however, show regions of local homogeneity. TEM images show that silver nanocrystals are well separated from those of copper and have a quasi-spherical shape, with an average diameter larger than that of copper nanocrystals. Vis–UV spectra showed the typical SPR of the nanostructured silver–copper glass–metal composites.

Some shards have drawings of blue smalt and yellow decorations made by a lead-antimonate pigment. It is observed that lustre nanocrystals are deposited, overlapped to a possible underlying pigment, when the pigment is finely dispersed in the glaze at low concentration. This occurs in the case of the cobalt blue drawings on the glaze. However, when yellow coloured decorations are obtained by large lead-antimonatecrystals, the formation of lustre nanocrystals is strongly hindered. Thus, a gold lustre is attained only at the border of the yellow decoration, where the large antimonate crystals are not present. Few silver crystals have been observed, by a careful SEM and TEM inspection, among the yellow pigment crystals at the surface of the glaze. However, their very low density does not allow to obtain any metallic lustre effect.

In terms of a simple model, suggested by the analogy of lustre and modern synthesized nanostructured metal–glass composites, the large antimonate crystals hinder lustre formation, possibly avoiding the initial penetration of silver and copper ions into the glaze. It is found that yellow lead-antimonate even hinders the crystallization of tin dioxide which, however, is normally present in the glaze as opacifier in the volume surrounding the pigmented region.

## References

[1] A. Caiger-Smith, Luster Pottery: Technique, Tradition and Innovation in Islam and the Western World, Faber and Faber, London, 1985.

[2] F. Amigues, M. Mesquida, Les Ateliers et la Céramique de Paterna, XIIIe–XIVe Siècles, Musée Saint-Jacques, Ville de Beziers, 1993.

[3] G. Busti, F. Cocchi, Museo Regionale della Ceramica di Deruta, Electa Editori Umbri Associati, Milano, 1999.

[4] G. Busti, in: C. Fiocco, G. Gherardi (Eds.), Ceramiche Umbre, Litografie Artistiche Faentine, Faenza, 1989.

[5] W.D. Kingery, P.B. Vandiver, Ceramic Masterpieces: Art, Structure and Technology, Free Press, New York, 1986, pp. 111–121.

[6] C. Piccolpasso, Li Tre Libri dell'Arte del Vasaio, 1557, Edizioni all'Insegna del Giglio, Firenze, 1976.

[7] J. Pérez-Arantegui, J. Molera, A. Larrea, T. Pradell, M. Vendrell-Saz, I. Borgia, B.G. Brunetti, F. Cariati, P. Fermo, M. Mellini, A. Sgamellotti, C. Viti, J. Am. Ceram. Soc. 84 (2001) 442.

[8] E.M. Vogel, J. Am. Ceram. Soc. 72 (1989) 719.

[9] G. De, M. Catalano, G. Battaglin, F. Caccavale, F. Gonella, P. Mazzoldi, R.F. Haglund, Appl. Phys. Lett. 68 (1996) 3820.

[10] C.R. Bamford, Colour Generation and Control in Glass, Elsevier, Amsterdam, 1977.

[11] R. Ashok (Ed.), Artists' Pigment: A Handbook of their History and Characteristics, National Gallery of Art, Washinghton, DC, 1997.

[12] A. Romani, C. Miliani, A. Morresi, N. Forini, G. Favaro, Appl. Surf. Sci. 157 (2000) 112.

[13] N. Gabrielli, F. Morresi, Proceedings of the Sixth International Conference on Non-destructive Testing and Microanalysis for the Diagnostics and Conservation of the Cultural and Environmental Heritage Art'99, Vol. 3, Rome, p. 2131.

[14] S. Volpin, A. Casoli, L. Alberici, Il colore ritrovato-Bellini a Venezia, Electa-Elemond Editori Associati, 2000, p. 175.

[15] I. Borgia, S. Bruni, B. Brunetti, C. Bianchi, F. Cariati, P. Fermo, A. Galli, G. Padeletti, A. Sgamellotti, in: A. Guarino (Ed.), Proceedings of the Second International Congress on Science and Technology for the Safeguard of Cultural Heritage in the Mediterranean Basin, Vol. 1, 2000, p. 441.

[16] M. Bacci, M. Picollo, Stud. Conserv. 41 (1996) 136.

[17] R.J. Gettens, G.L. Stout, Painting Materials: A Short Encyclopaedia, Dover, New York, 1965.

[18] J. Molera, T. Pradell, N. Salvadó, M. Vendrell-Saz, J. Am. Ceram. Soc. 82 (1999) 2871.

[19] R.H. Magruder III, D.H. Osborne Jr., R.A. Zuhr, J. Non-Cryst. Solids 176 (1994) 299.

[20] G. De, M. Gusso, L. Tapfer, M. Catalano, F. Gonella, G. Mattei, P. Mazzoldi, G. Battaglin, J. Appl. Phys. 80 (1996) 6734.

[21] E. Borsella, E. Cattaruzza, G. De Marchi, F. Gonella, G. Mattei, P. Mazzoldi, A. Quaranta, G. Battaglin, R. Polloni, J. Non-Cryst. Solids 245 (1999) 122.

[22] F. Gonella, Nucl. Instrum. Meth. B 166–167 (2000) 831.

[23] G. De, M. Gusso, L. Tapfer, M. Catalano, G. Battaglin, F. Caccavale, F. Gonella, P. Mazzoldi, J. Appl. Phys. 80 (1996) 6734.

[24] A. Miotello, G. De Marchi, G. Mattei, P. Mazzoldi, A. Quaranta, Appl. Phys. A 67 (1998) 527.

[25] R. Bertoncello, F. Trivillin, E. Cattaruzza, P. Mazzoldi, G.W. Arnold, G. Battaglin, M. Catalano, J. Appl. Phys. 77 (1995) 1294.

[26] A. Miotello, G. De Marchi, G. Mattei, P. Mazzoldi, A. Quaranta, Appl. Phys. A 70 (2000) 415.